

The profile of an oil-water interface in a spin-up rotating cylindrical vessel

Zixiang Yan, Lu Sun, Jinghua Xiao, and Yueheng Lan

Citation: [American Journal of Physics](#) **85**, 271 (2017); doi: 10.1119/1.4975125

View online: <https://doi.org/10.1119/1.4975125>

View Table of Contents: <http://aapt.scitation.org/toc/ajp/85/4>

Published by the [American Association of Physics Teachers](#)

Articles you may be interested in

[The Ewald sphere construction for radiation, scattering, and diffraction](#)
American Journal of Physics **85**, 277 (2017); 10.1119/1.4973369

[Relating Brownian motion to diffusion with superparamagnetic colloids](#)
American Journal of Physics **85**, 265 (2017); 10.1119/1.4975382

[Why trains stay on tracks](#)
American Journal of Physics **85**, 178 (2017); 10.1119/1.4973370

[Weight of an hourglass—Theory and experiment in quantitative comparison](#)
American Journal of Physics **85**, 98 (2017); 10.1119/1.4973527

[Sliding down an arbitrary curve in the presence of friction](#)
American Journal of Physics **85**, 108 (2017); 10.1119/1.4966628

[A quantitative analysis of the chain fountain](#)
American Journal of Physics **85**, 414 (2017); 10.1119/1.4980071



American Association of **Physics Teachers**

Explore the **AAPT Career Center** – access hundreds of physics education and other STEM teaching jobs at two-year and four-year colleges and universities.

<http://jobs.aapt.org>

The profile of an oil-water interface in a spin-up rotating cylindrical vessel

Zixiang Yan^{a)}

School of Science, Beijing University of Posts and Telecommunications, Beijing 100876, China

Lu Sun

School of Information and Communication Engineering, Beijing University of Posts and Telecommunications, Beijing 100876, China

Jinghua Xiao^{b)} and Yueheng Lan

School of Science, Beijing University of Posts and Telecommunications, Beijing 100876, China

(Received 27 August 2015; accepted 16 January 2017)

The dynamics of a two-layered rotating liquid at low angular velocity in a cylindrical container is explored, both experimentally and theoretically, using an oil-water system. In the two-layered liquid, a transient concave down paraboloid interface, containing undulations, is observed before the final, stable concave up paraboloid interface develops. A simple yet effective model is developed to explain the observed profile dynamics, in which the predicted maximal height of the paraboloid agrees well with experimental measurements over a fairly large range of rotation speeds. © 2017 American Association of Physics Teachers.

[<http://dx.doi.org/10.1119/1.4975125>]

I. INTRODUCTION

Rotating liquids have been studied for more than four hundred years since the discussion of Newton's rotating bucket in the 1600s, when the observed stable paraboloid profile was well characterized scientifically. Since then, research interest has been focused on the static and dynamic processes that could appear in rotating liquids. In the investigation of static states, refined models for single-component rotating liquids and their profiles were developed by Goodman,² Sabatka and Dvorak,³ Turkington and Osborne,⁴ Lubarda,⁵ and Bergmann *et al.*⁶ Interesting surface profiles of single-component liquids are measured experimentally and discussed in college-level courses on physics.^{11,12} One of the applications of the surface shape is to large astronomical telescopes, where rotating liquid can be used as focal-length adjustable parabolic mirror.^{7,16} On the more fundamental side, there have also been studies of the rotating liquid's dynamic behavior, such as the spin-up phenomenon of rotating liquids in a cylindrical container,^{1,17,18} as well as the motion of a rotating layer at the boundary⁸ and at the bottom of the container.⁹ Recent results of Wan *et al.*¹⁰ showed that the attenuation of the angular velocity of single-component liquids in a cylindrical container is due to the boundary friction, while turbulence energy loss can actually be ignored. This result will be effectively invoked in our work.

The phenomena are more complicated for two-layered liquids since the two liquids usually have different densities or viscosities; this may lead to differences in response time and thus interesting transient behavior could arise. Much work has been done to study the dynamics of the interface between the two liquids. Yoshikawa and Wesfreid confirmed the existence of the Kelvin-Helmholtz waves in a system undergoing torsional oscillations.¹³ Baker demonstrated a greatly magnified concave up paraboloid at the interface between a rotating lower fluid and a stationary upper fluid.¹ In his study of the dynamics of spin-up and spin-down, Baker¹ noted that if the proper conditions are satisfied, the

interface of the two-layered liquid could form a concave down paraboloid (a dome) in the spin-up process, a remarkably different outcome from the concave up paraboloid routinely appearing in a rotating liquid. Whether this really happens, or whether any other unexpected fluid behavior can be observed, awaits an experimental demonstration and a detailed theoretical explanation.

Our study here is concentrated on the profile of the oil-water interface in the spin-up process. With both experimental observation and theoretical computation, we find that the evolution of the interfacial profile is regulated by the gradually changing angular velocity of the water during the spin-up process. The theoretical model makes a prediction of the maximal height of the concave down paraboloid, a prediction that agrees well with the experimental measurements over quite a broad range of rotation speeds.

The rest of this paper is organized as follows. In Sec. II, the experimental details are described. Theoretical development of the model and experimental comparison are presented in Sec. III. Finally, in Sec. IV, we provide a brief summary.

II. DESCRIPTION OF THE EXPERIMENT

A. Experimental set-up

Figure 1 displays the experimental apparatus (FB805, made by Jingke, Hangzhou, China) for the rotating liquid used in the current experiment and in studies of a single-component rotating liquid. The apparatus consists of an electric rotor that controls the angular velocity ω_v of a vessel and can be continuously adjusted from 24 to 146 revolutions per minute; a ruler; a pedestal holding a glass beaker of radius $R = 0.0522 \pm 0.0004$ m containing oil and water; and a photogate measuring the period of the beaker's rotation. The maximal height of the concave down paraboloid interface is measured using the ruler, while the angular velocity of the beaker is read from the photogate. At rest, the heights of oil

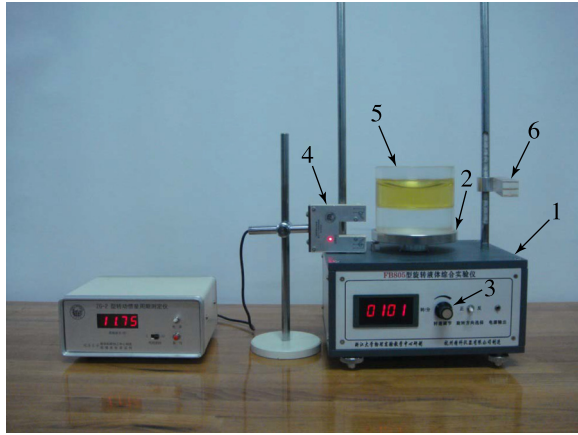


Fig. 1. Experimental setup (1: electric rotor; 2: pedestal; 3: velocity control knob; 4: photogate; 5: glass beaker with oil and water; 6: ruler).

and water are $H_o = 0.0470$ m and $H_w = 0.0255$ m. The oil used in the experiment is castor oil produced by Cool Chemical Science and Technology (Beijing) Co. LTD, having a density $\rho_o = 0.94 \times 10^3$ kg/m³ and viscosity $\mu_o = 0.62$ Pa s, as specified in the manual for the product. The oil is freshly extracted from the bottom of its original sealed container for each experiment in order to minimize any aging effects. The density of water is $\rho_w = 1.00 \times 10^3$ kg/m³ and its viscosity is $\mu_w = 8.9 \times 10^{-4}$ Pa s. It will be shown below that uncertainty in these parameter values has only a minor influence on the experimental results.

B. Phenomena during the spin-up process

In comparison to single-component liquids, several new interesting phenomena, displayed in Fig. 2, are observed in the spin-up process of two-layered rotating liquids. In the following, we will pay special attention to the evolution of the upper surface and the lower interface of the bulk oil.

When the cylindrical container spins up from a stationary state, the upper surface of oil becomes concave up immediately (in less than a second). However, the oil-water interface curves oppositely, as shown in Fig. 2(a); this can be attributed to the difference in the transient angular velocities of the water and the oil. This parabolic interface soon attains a maximal height and continues to maintain its shape for 1–2 s, as displayed in Fig. 2(b). After this time, undulations on the surface start to appear, as shown in Fig. 2(c), indicating an impending qualitative change of the interface. The interface then changes to its stable shape of a concave up paraboloid, as shown in Fig. 2(d). [We use a larger angular velocity in Fig. 2(d) in order to show the interface more clearly.]

We note that during the spin-up process, it is easy to see the build-up of the concave down paraboloid. As mentioned, its maximal height is maintained for about 1–2 s [Fig. 2(b)] before decaying and hence is easy to measure, thus providing an excellent feature to verify our theoretical model.

Timescale separation in the buildup of the rotation of the oil and the water underlies the previous observations. The rotation of the oil is mainly caused by the sidewall of the vessel, with a timescale $\tau_o \sim (\rho_o/\mu_o)R^2 \sim 4.1$ s, whereas the water is spun up by both the sidewall and the bottom of the vessel, and has a characteristic time $\tau_w \sim (\rho_w/\mu_w)R^2 = 3061$ s. Hence, τ_w is nearly three orders of magnitude larger than τ_o , and we expect

an inviscid spin-up process for the water and a viscous spin-up process for the oil at small time scales.

As displayed in Fig. 2, the concave down paraboloid emerges several seconds after the start, a time much smaller than τ_w , the necessary time to build up the boundary layer for the water. Henceforth, the water can be viewed as an inviscid fluid with a negligible boundary layer in the first few seconds; this will be used to simplify our theoretical analysis.

As a result of the above considerations, the entire process can be divided into two steps: the spin-up process of the oil and that of the water. The first one is a fast process because oil has a large viscosity. Hence, oil quickly acquires the angular velocity of the container and its upper surface reaches a stationary shape within a short time, in a process that is well described by the theory of a single-component rotating liquid.² In the second step, the rotation of the water is slowly built up, due to water's small viscosity. With the speed-up of the rotation, the oil-water surface becomes unstable and keeps changing its profile until a stable concave up paraboloid finally forms.

III. THEORETICAL ANALYSES

A. A modified model adapted to the two-layered liquid

We start from the model of a single-component liquid (suppose it is the oil), which is described as an incompressible rotating potential flow.¹⁴ We take as characteristic scales $[L] = R$, $[p] = \rho_o g R$, $[\rho] = \rho_o$, and $[\omega] = (g/R)^{1/2}$, where g is the gravitational field strength. Unless stated otherwise we use these characteristic scales to write variables in dimensionless form. In a frame corotating with the container, the pressure inside the liquid can be obtained from the force balance condition

$$p = p_0 + Z_o - h + \frac{1}{2} \omega^2 r^2, \quad (1)$$

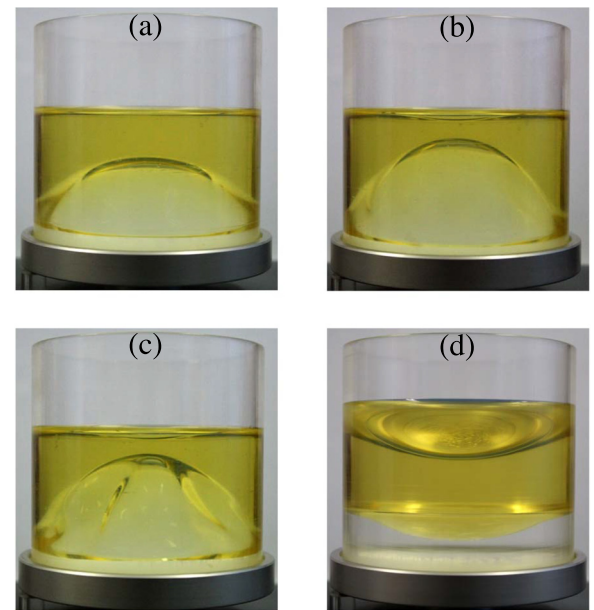


Fig. 2. Temporal progression of the interface in the two-layered liquid during the spin-up process (side view): $\omega_v = 6.28$ rad/s at times (a) $t = 0.8$ s, (b) $t = 2.0$ s, and (c) $t = 3.2$ s; (d) $\omega_v = 12.04$ rad/s at time $t = 80.0$ s.

where p_0 is the atmospheric pressure, r is the horizontal distance from the rotation axis, h is the vertical distance from the bottom of the container, and Z_o represents the height of the lowest point of the liquid surface. Rigorously speaking, Eq. (1) only applies to fluid in a steady state with constant angular velocity ω . As can be seen from Eq. (1), the shape of the free surface of the rotating liquid is a paraboloid.

In the corotating frame displayed in Fig. 3(a), where Z_o and Z_c denote, respectively, the heights of the lowest point and an arbitrarily point on the surface, force balance leads to

$$Z_c - Z_o = \frac{1}{2} \omega^2 r^2, \quad (2)$$

which gives the shape of a paraboloid. The height of the lowest point Z_o can be further expressed as a function of the height H of the liquid at rest by the conservation of volume,

$$\int_0^1 H(2\pi r) dr = 2\pi \int_0^1 \left(\frac{1}{2} \omega^2 r^2 + Z_o \right) r dr, \quad (3)$$

giving

$$Z_o = H - \frac{1}{4} \omega^2. \quad (4)$$

During the acceleration, the angular velocity ω is not the same at every point in the liquid. However, as shown by Baker,¹ the radial and axial velocity components of the flow at low angular velocity are far smaller than the azimuthal velocity, and the variation of ω along r is also small; Eq. (1) is thus still a good approximation.

Figure 3(b) depicts the concave down paraboloid at the oil-water interface, where Z_a denotes the height of the paraboloid apex, and Z_b the height of an arbitrary point on the interface. The shape of the upper surface of the oil can still be represented by Eq. (2) so that one can write

$$Z_c - Z_o = \frac{1}{2} \omega_o^2 r^2. \quad (5)$$

Since the fluid is nearly hydrostatic and all the forces are horizontal except gravity, the pressure in the oil can be written as

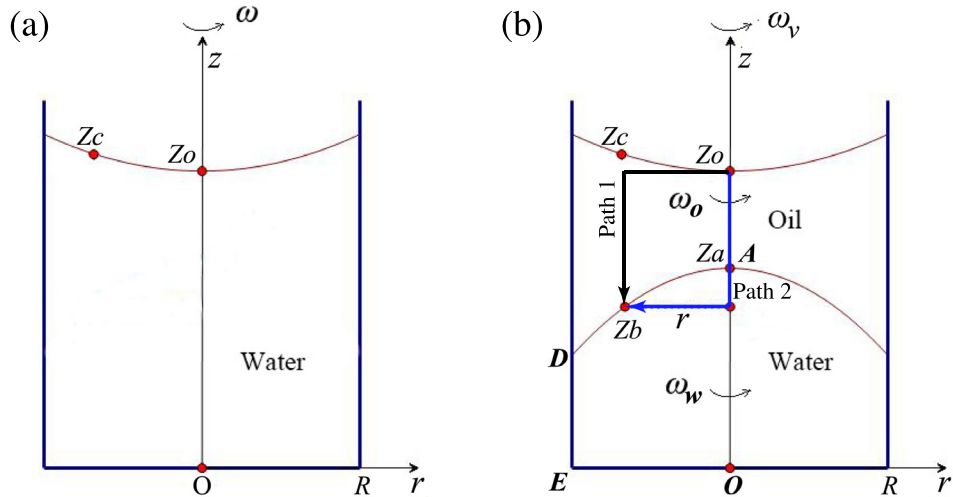


Fig. 3. Schematic drawing of the rotating liquid experiment: (a) a single liquid; (b) the two-liquid situation.

$$p - p_0 = -(h - Z_o) + \frac{1}{2} \omega_o^2 r^2. \quad (6)$$

Therefore, along path 1 in Fig. 3(b) we have

$$p_b - p_0 = -(Z_b - Z_o) + \frac{1}{2} \omega_o^2 r^2, \quad (7)$$

whereas on path 2 it is

$$p_b - p_0 = Z_o - Z_a + \rho_w (Z_a - Z_b) + \frac{1}{2} \rho_w \omega_w^2 r^2. \quad (8)$$

Combining Eqs. (7) and (8) and introducing the (dimensionless) Atwood number A , defined in terms of dimensional variables as $A = (\rho_w - \rho_o)/(\rho_w + \rho_o)$, the difference between Z_a and Z_b becomes

$$\Delta h = Z_a - Z_b = \frac{(1 - A)\omega_o^2 - (1 + A)\omega_w^2}{4A} r^2. \quad (9)$$

In terms of the original (dimensional) variables, Eq. (9) reads $\Delta h = (\rho_o \omega_o^2 - \rho_w \omega_w^2) r^2 / [2(\rho_w - \rho_o)g]$. According to the analysis in Sec. III B, the inverted dome will appear only when $A > 0$, otherwise the interface will be flat (when $A = 0$) or the normal paraboloid (when $A < 0$). In Baker's work,¹ the equation describing the paraboloid is our Eq. (9) at $\omega_o = 0$. (Note that in his work $\Delta h = Z_b - Z_a$).

As in Baker's work, we study a situation in which one of the fluids is essentially at rest, while the other is rotating with the vessel. However, unlike Baker, we also consider the spin-up process and the evolution of the profile of the oil-water interface.

B. The angular velocity of water and its influence

Because oil reaches its stationary state in a very short time, the upper layer assumes the steady concave up paraboloid long before the oil-water interface gets stabilized. Therefore, the angular velocity (ω_o) of the oil soon becomes approximately equal to that of the vessel (ω_v).

For our purpose, the water can be treated as an inviscid fluid,¹⁴ i.e., the angular velocity (ω_w) is regarded as constant in the bulk but has a jump at the boundary. In general, this

approximation is good, but subtle deviations can still be observed. For example, transient drapes caused by Kelvin-Helmholtz instabilities at the interface, as displayed in Fig. 2(c), are observed in the spin-up process. The analysis of such instabilities is beyond the scope of this work.

It takes about 2 s for the oil-water interface to reach its maximal height if $\omega_w < 6$ rad/s, which is the maximum speed of the electric rotor. Compared with the overall relaxation time (about 40–60 s), we conclude that ω_w is much smaller than ω_o during the first few seconds, and that as a first approximation one can assume $\omega_w = 0$. The height of the oil-water interface can then be obtained by setting $r = R$ in Eq. (9), written here in terms of the original, dimensional variables

$$\Delta h_{\max} = \frac{(\rho_o \omega_o^2 - \rho_w \omega_w^2) R^2}{2(\rho_w - \rho_o) g} \approx \frac{(\rho_o \omega_o^2) R^2}{2(\rho_w - \rho_o) g}. \quad (10)$$

Figure 4 shows a comparison between the theoretical results (solid curve) given in Eq. (10) and experimental measurements for ω_v between 2.3 rad/s and 5.3 rad/s. The discrepancies increase from 4% at $\omega_v = 2.3$ rad/s to 20% at $\omega_v = 5.3$ rad/s. Results below 2.3 rad/s are not displayed in the figure as the errors are generally less than 4%. The large deviation at high angular velocity may be accounted for by the nonzero ω_w at the maximal height.

C. Derivation of ω_w as a function of time

The shear force on the oil-water interface is neglected in our analysis because the interaction between two insoluble liquids is small in a container of size $R = 0.0522 \pm 0.0004$ m. Thus, the dragging force from the wall and the bottom of container becomes the main driver in the spin-up process.

From volume conservation, one obtains

$$V_w = \pi H_w = 2\pi \int_0^1 r \left[Z_a - \frac{(1-A)\omega_o^2 - (1+A)\omega_w^2}{4A} r^2 \right] dr, \quad (11)$$

$$V_o = \pi H_o = 2\pi \int_0^1 r \left[\frac{1}{2} \omega_o^2 r^2 + Z_o - Z_a + \frac{(1-A)\omega_o^2 - (1+A)\omega_w^2}{4A} r^2 \right] dr, \quad (12)$$

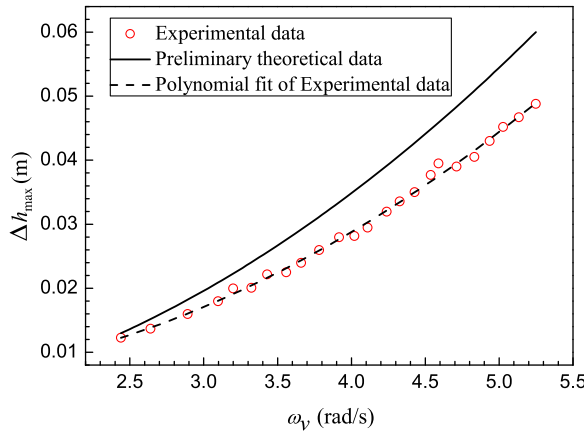


Fig. 4. The maximum height of the concave down paraboloid as a function of angular velocity; experimental results and theoretical computation.

where V_w and V_o represent the volume of water and oil, respectively. Combining Eqs. (11) and (12) then gives the values of Z_b and Z_c

$$\begin{aligned} Z_b &= Z_a - \frac{(1-A)\omega_o^2 - (1+A)\omega_w^2}{4A} r^2 \\ &= H_w + \frac{(1-A)\omega_o^2 - (1+A)\omega_w^2}{8A} \\ &\quad - \frac{(1-A)\omega_o^2 - (1+A)\omega_w^2}{4A} r^2, \end{aligned} \quad (13)$$

and

$$\begin{aligned} Z_c &= Z_o + \frac{1}{2} \omega_o^2 r^2 \\ &= H_o + H_w - \frac{1}{4} \omega_o^2 + \frac{1}{2} \omega_o^2 r^2. \end{aligned} \quad (14)$$

Meanwhile, the total kinetic energy of the rotating fluids is

$$\begin{aligned} E_k &= \frac{1}{2} \int_0^1 2\pi r (Z_c - Z_b) \omega_o^2 r^2 dr \\ &\quad + \frac{1+A}{2(1-A)} \int_0^1 2\pi r Z_b \omega_w^2 r^2 dr, \end{aligned} \quad (15)$$

and the total gravitational potential energy is

$$\begin{aligned} E_h &= \int_0^1 2\pi r (Z_c - Z_b) \frac{Z_c + Z_b}{2} dr \\ &\quad + \frac{1+A}{1-A} \int_0^1 2\pi r Z_b \frac{Z_b}{2} dr. \end{aligned} \quad (16)$$

Since the shear force at the interface is neglected, any decrease of the total energy is mainly caused by the drag from the wall and the bottom of the container. When the angular velocity of the oil is equal to that of the container, i.e., when $\omega_o = \omega_v$, the energy dW_1 dissipated at the wall in a time dt is¹⁴

$$\begin{aligned} dW_1 &= -2\pi R z_R \tau_w v(R) dt \\ &= -\frac{\lambda}{4} \pi \frac{1+A}{1-A} (\omega_w - \omega_v)^3 \\ &\quad \times \left[H_w - \frac{(1-A)\omega_o^2 - (1+A)\omega_w^2}{8A} \right] dt, \end{aligned} \quad (17)$$

and the energy dW_2 dissipated at the bottom is

$$\begin{aligned} dW_2 &= - \int_0^1 2\pi r dr \tau_w v(r) dt \\ &= -\frac{\lambda}{4} \pi \frac{1+A}{1-A} (\omega_w - \omega_v)^3 \frac{1}{5} dt. \end{aligned} \quad (18)$$

In these equations, the velocity is $v(r) = \omega r$, the wall shear is $\tau_w = \lambda \rho v(r)^2 / 8$, z_R is the length of segment DE in Fig. 3(b), and λ is a friction damping factor that will be given momentarily. The power dissipation should be equal to the rate of the change of the total energy, and thus,

$$\frac{d(W_1 + W_2)}{dt} = \frac{\partial(E_k + E_h)}{\partial \omega_w} \frac{d\omega_w}{dt}. \quad (19)$$

Inserting Eqs. (15)–(18) into Eq. (19), one finally derives the rate of change of ω_w . In terms of the original dimensional variables the result is

$$\frac{d\omega_w}{dt} = -\frac{\lambda}{2} \frac{(\omega_w - \omega_v)^3}{\omega_w} \times \left\{ 1 + \frac{R}{5} \left[H_w - \frac{\rho_o \omega_o^2 - \rho_w \omega_w^2}{4(\rho_w - \rho_o)g} R^2 \right]^{-1} \right\}. \quad (20)$$

The drag of the container changes with ω_w , and the spin-up process can be approximately divided into three regimes: the laminar regime, the hydraulically smooth regime, and the hydraulically rough regime. The friction loss comes from the drag of the wall and the bottom, similar to that for flow in pipes.¹⁴ Thus, the friction loss factor

λ has a similar dependence on the Reynolds number Re . In terms of the original (dimensional) variables, the Reynolds number is defined as $Re = v_a d / \nu$, where $v_a = 2(\omega_v - \omega_w)R/3$ is the average local velocity and $\nu = 8.9 \times 10^{-7} \text{ m}^2/\text{s}$ is the kinematic viscosity. Note that the average local velocity defined here is the *relative* velocity between the water and the container, which leads to a rather different definition of the Reynolds number than is typical. For example, when the water is moving very slowly there is a large relative velocity between the water and the container, and hence a large Reynolds number. Based on a fitting to experimental data,¹⁰ the friction loss factor can be written as the piecewise function

$$\lambda = \begin{cases} 1 / \left[\lg(3.7d/\Delta)^2 \right]^2 & Re_c < Re \quad (\text{the laminar regime}) \\ 0.316 / Re^{1/4} & 2300 < Re < Re_c \quad (\text{the hydraulically smooth regime}) \\ 64 / Re & Re < 2300 \quad (\text{the hydraulically rough regime}), \end{cases} \quad (21)$$

where $Re_c = 10d/\Delta$ is the critical Reynolds number distinguishing the hydraulically smooth regime from the laminar regime. In this expression, $\Delta = 10 \mu\text{m}$ refers to the wall roughness height while d is the pipe diameter. In this situation, the pipe diameter can be written as $d = 4R_n$, where the hydraulic radius R_n can be calculated (using dimensional variables) using Fukuchi's formula¹⁵

$$R_n = \left[H_w R + \frac{(\rho_o \omega_o^2 - \rho_w \omega_w^2)}{12(\rho_w - \rho_o)g} R^3 \right] / \left[R + H_w - \frac{(\rho_o \omega_o^2 - \rho_w \omega_w^2)}{4(\rho_w - \rho_o)g} R^2 \right]. \quad (22)$$

Note that the Reynolds number Re plays a very important role in this two-layer situation. If it is too small, the observed concave down paraboloid may not appear at all. However, the exact value of the Reynolds number at which the paraboloid first appears is not determined in the current investigation. Here, for simplicity we assume that oil immediately acquires the angular velocity of the vessel. The actual detailed dynamical process and its dependence on various parameters would require further research and is beyond the scope of this work.

D. Comparison with experiments

Based on the Reynolds number Re of the water for different angular velocities, we find that the water is in the hydraulically smooth regime from the beginning to around 2 s, when the oil-water interface reaches its maximal height. Thus, with ω_v replacing ω_o , numerical integration of Eq. (20) gives the results displayed in Fig. 5 for various angular velocities of the container ω_v , when the water is in the hydraulically smooth regime. The squares in Fig. 5, magnified in the inset, display the values of ω_w at the moment that

the interface reaches the maximal height (time is measured by a stop watch in the experiment). Inserting ω_w read from Fig. 5 into Eq. (9), one can obtain a refined theoretical result for Δh_{\max} (see Fig. 6). As shown in Fig. 6, the refined model is an improvement compared to the result assuming $\omega_w = 0$ (displayed in Fig. 4). The relative error is less than 10% when the measured angular velocity of the container is less than about 4.10 rad/s, which shows the effectiveness of our simplified model.

However, this model could still be improved in the regime where the angular velocity of the container is greater than about 4.10 rad/s. As shown in Fig. 6, the discrepancy between experiment and theory increases as the angular velocity of the container increases, which implies that our simplification, $\omega_o = \omega_v$, is no longer valid. The spin-up process of the water would be faster than the model computation

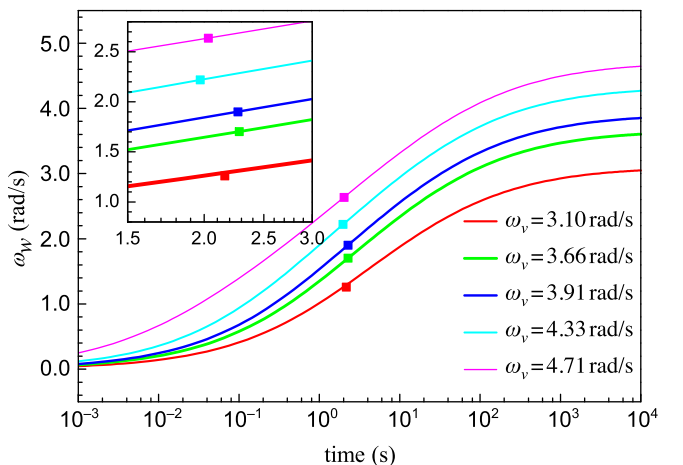


Fig. 5. The change of ω_w with time in the hydraulically smooth regime. From bottom to top, the curves have $\omega_v = 3.10, 3.66, 3.91, 4.33$, and 4.71 rad/s , respectively. The squares display the values of ω_w at the moment that the interface reaches the maximal height.

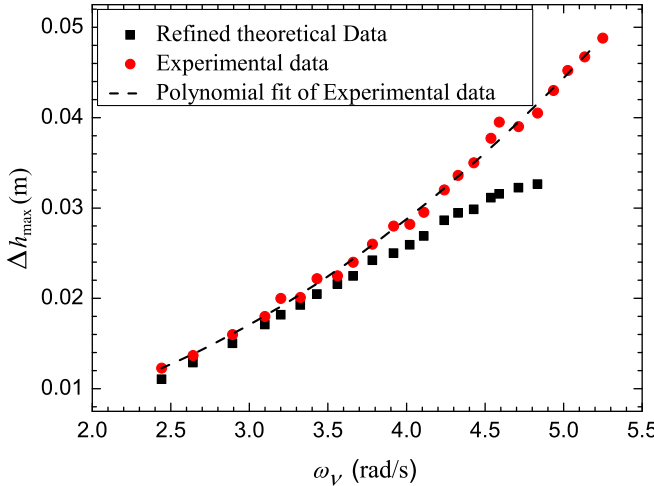


Fig. 6. Comparison of experimental heights and refined theoretical heights.

as the angular velocity of the container becomes greater. The simplification in our model is invalid when the spin-up time of the water is comparable to that of the oil. If we continue using $\omega_o = \omega_v$ at large values of ω_v , the spin-up process of the water will be faster than expected according to Eq. (20), and this would render the value of the predicted height from Eq. (9) smaller than the real height, as shown in Fig. 6.

In addition, our assumption of essentially rigid behavior in the fluids might also no longer be valid. The angular velocities may vary with both h and r in the real fluid and may change in a spatially non-uniform way. The investigation of this complication is beyond the scope of the current paper, and is left for a future, more detailed study.

IV. SUMMARY

We have investigated the profile of the oil-water interface in the spin-up process with experiments and theoretical models. The transient concave down paraboloid and its maximal height are described using a simplified hydrodynamic model. The change of the profile is mainly attributed to the variation of angular velocity of water during the spin-up process. A theoretical model is built on this observation, and that model is shown to produce results in reasonably good agreement with experimental measurements; the discrepancy between experiment and theory is less than 10% for $\omega_v \lesssim 4.10$ rad/s. Our investigation will be beneficial to similar computations of the interface of two-layered liquids rotating in a

cylindrical container, as well as to two-layered ocean currents with different chemical properties.

ACKNOWLEDGMENTS

This work was supported by the National College Innovation Program of Beijing University of Posts and Telecommunications and the Fundamental Research Funds for the Central Universities. The authors would like to thank Dr. Wei Kang and Dr. Hujiang Yang for their helpful suggestions.

^aElectronic mail: yanzx@bupt.edu.cn

^bElectronic mail: jhxiao@bupt.edu.cn

¹D. J. Baker, Jr., “Demonstrations of fluid flow in a rotating system II: The ‘Spin-Up’ problem,” *Am. J. Phys.* **36**, 980–986 (1968).

²J. M. Goodman, “Paraboloids and vortices in hydrodynamics,” *Am. J. Phys.* **37**, 864–868 (1969).

³Z. Sabatka and L. Dvorak, “Simple verification of the parabolic shape of a rotating liquid and a boat on its surface,” *Phys. Educ.* **45**(5), 462–468 (2010).

⁴R. R. Turkington and D. V. Osborne, “On the influence of surface tension on the surface profile of a rotating liquid,” *Proc. Phys. Soc.* **82**, 614–619 (1963).

⁵V. A. Lubarda, “The shape of a liquid surface in a uniformly rotating cylinder in the presence of surface tension,” *Acta Mech.* **224**, 1365–1382 (2013).

⁶R. Bergmann *et al.*, “Polygon formation and surface flow on a rotating fluid surface,” *J. Fluid Mech.* **679**, 415–431 (2011).

⁷R. E. Berg, “Rotating liquid mirror,” *Am. J. Phys.* **58**, 280–281 (1990).

⁸E. J. Hitch, M. A. Kelmanson, and P. D. Metcalfe, “Shock-like free-surface perturbations in low-surface-tension, viscous, thin-film flow exterior to a rotating cylinder,” *Phys. Eng. Sci.* **460**, 2975–2991 (2004).

⁹M. Piva and E. Meiburg, “Steady axisymmetric flow in an open cylindrical container with a partially rotating bottom wall,” *Physics of Fluids* **17**, 063603 (2005).

¹⁰W. Wan, Y. Yu, and H. Bai, “Investigation on the attenuation of a rotating liquid motion in a cylinder with boundary resistance,” *Chinese Journal of Theoretical and Applied Mechanics* **46**(4), 505–511 (2014).

¹¹PHYWE, “Surface of rotating liquids” laboratory experiment, available online at <<https://www.phywe.com/en/surface-of-rotating-liquids.html>>.

¹²M. Basta, V. Picciarelli, and R. Stella, “A simple experiment to study parabolic surfaces,” *Phys. Educ.* **35**(2), 120–123 (2000).

¹³H. Yoshikawa and J. E. Wesfreid, “Oscillatory Kelvin-Helmholtz instability. Part 2. An experiment in fluids with a large viscosity contrast,” *J. Fluid Mech.* **675**, 249–267 (2011).

¹⁴F. M. White, *Fluid Mechanics*. 4th ed. (McGraw-Hill, New York, NY, 2001), pp. 93–95, 326–342.

¹⁵T. Fukuchi, “Hydraulic Elements chart for pipe flow using new definition of hydraulic radius,” *Hydraulic Eng.* **132**(9), 990–994 (2006).

¹⁶P. Klimas *et al.*, “Lunar liquid mirror telescope: structural concepts,” *Proc. SPIE* **7732**, 77322U (2010).

¹⁷J. R. Holton and P. H. Stone, “A note on the spin-up of a stratified fluid,” *J. Fluid Mech.* **33**, 127–129 (1968).

¹⁸J. B. Flor, M. Ungarish, and J. W. M. Bush, “Spin-up from rest in a stratified fluid: Boundary flows,” *J. Fluid Mech.* **472**, 51–82 (2002).